ELSEVIER

Remote Sensing of Environment 83 (2002) 149–162

Remote Sensing of Environment

www.elsevier.com/locate/rse

Validating MODIS land surface reflectance and albedo products: methods and preliminary results

Shunlin Liang [a,*], Hongliang Fang [a], Mingzhen Chen [a], Chad J. Shuey [a], Charlie Walthall [b], Craig Daughtry [b], Jeff Morisette [c], Crystal Schaaf [d], Alan Strahler [d]

[a] *Laboratory of Global Remote Sensing Studies, Department of Geography, University of Maryland, 2181 LeFrak Hall, College Park, MD 20742, USA*

[b] *Hydrology and Remote Sensing Laboratory, USDA Agriculture Research Service, Beltsville, MD, USA*

[c] *Biospheric Science Branch, NASA Goddard Space Flight Center, Greenbelt, MD, USA*

[d] *Department of Geography and Center for Remote Sensing, Boston University, Boston, MA, USA*

Received 23 April 2001; received in revised form 4 January 2002; accepted 8 February 2002

Abstract

This paper presents the general methods and some preliminary results of validating Moderate-Resolution Imaging Spectroradiometer (MODIS) land surface reflectance and albedo products using ground measurements and Enhanced Thematic Mapper Plus (ETM+) imagery. Since ground "point" measurements are not suitable for direct comparisons with MODIS pixels of about 1 km over heterogeneous landscapes, upscaling based on high-resolution remotely sensed imagery is critical. In this study, ground measurements at Beltsville, MD were used to calibrate land surface reflectance and albedo products derived from ETM+ imagery at 30 m, which were then aggregated to the MODIS resolution for determining the accuracy of the following land surface products: (1) bidirectional reflectance from atmospheric correction, (2) bidirectional reflectance distribution function (BRDF), (3) broadband albedos, and (4) nadir BRDF-adjusted reflectance. The initial validation results from ground measurements and two ETM+ images acquired on October 2 and November 3, 2000 showed that these products are reasonably accurate, with typically less than 5% absolute error. Final conclusions on their accuracy depend on more validation results.

1. Introduction

Moderate-Resolution Imaging Spectroradiometer (MODIS) is the primary sensor for monitoring the terrestrial ecosystem for the NASA Earth Observing System (EOS) program at the resolution of 250–1000 m. There are a series of high-level land surface products that are being generated by the MODIS land science team (Justice, Vermote, et al., 1998). We performed the initial validation of the following land surface products in this study: (1) bidirectional reflectance product from atmospheric correction (MOD09) (Vermote, 1999), (2) bidirectional reflectance distribution function (BRDF) (MOD43B1) (Strahler et al., 1999), (3) broadband albedos (MOD43B3) (Strahler et al., 1999), and (4) nadir BRDF-adjusted reflectance (MOD43B4) (Schaaf et al., 2002).

Validating these land surface products is important because their accuracy is critical to the scientific community for various applications. Any feedback from the validation activity will also help improve the generation of these products.

Satellite product validation has to rely on surface measurements through field campaigns. However, validating MOD09 and MOD43 products using ground measurements is very challenging. One of the major problems is the scale mismatch between ground "point" measurements and the MODIS resolutions. Unless the surface is large and perfectly homogeneous or a sufficient number of point measurements can be made during the satellite overpass, "point" measurements may not be sufficient to validate the 1-km MODIS products if direct comparison is employed. Therefore, upscaling from ground "point" measurements to the MODIS resolutions using high-resolution remotely sensed imagery is a necessary and critical step. This is illustrated in Fig. 1. The ground measurements are used to "calibrate" the products from high-resolution imagery, which are then aggregated to the MODIS resolutions. In this paper, we

* Corresponding author. Tel.: +1-301-405-4556; fax: +1-301-314-9299.
E-mail address: sliang@geog.umd.edu (S. Liang).

0034-4257/02/$ - see front matter © 2002 Elsevier Science Inc. All rights reserved.
PII: S0034-4257(02)00092-5

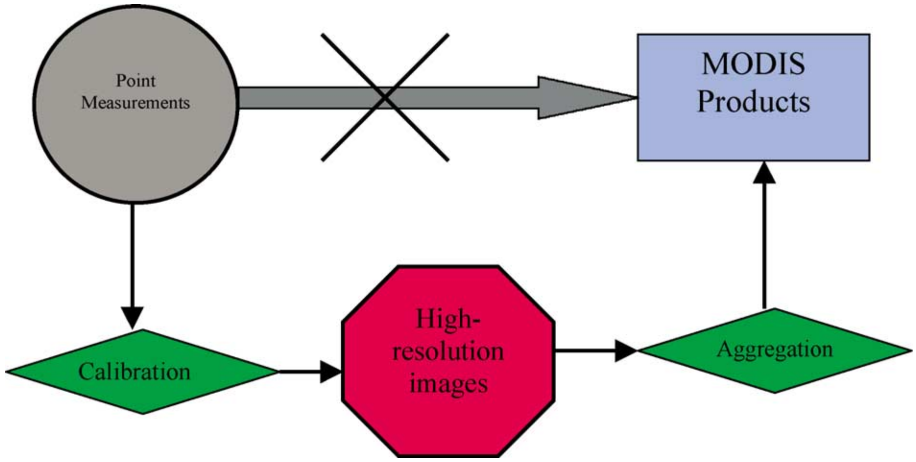

Fig. 1. Illustration of the validation strategy.

focus mainly on the upscaling methods and some preliminary validation results. The methodology should be equally useful for other validation sites and/or validating similar land surface products of other environmental satellite systems.

2. Field campaign and ground measurement

A series of field campaigns were conducted over the last few years to measure surface radiometric quantities over the USDA Agricultural Research Service Beltsville Agricultural Research Center (BARC) in Beltsville, MD, USA. This site is located northeast of Washington, DC and is adjacent to the NASA Goddard Space Flight Center (GSFC). The central geographic location is (39.03°N, 76.85°W). Most measurements were made in a region of about 10×10 km around this central location—an area of diverse soils, crops, natural vegetation covers, and man-made objects. This validation site has been identified as one of 24 NASA EOS Land Validation Core Sites (Justice, Starr, Wickland, Privette, & Suttles, 1998; Morisette, Privette, & Justice, 2002; Morisette et al., 1999). In this region, Sunphotometers installed at NASA/GSFC as part of the AERONET system (Holben et al., 1998) provide continuous measurements of the aerosol optical depth and column water vapor content of the atmosphere. Ground measurements for our validation purposes mainly include surface reflectance spectra of a variety of cover types measured with an Analytical Spectral Device (ASD) spectroradiometer (covering the spectrum of 0.35–2.5 μm) and broadband albedos measured using Kipp and Zonen CM21 albedometers (see Fig. 2). The broadband albedos (total-shortwave, -visible and -near-infrared) were measured using two albedometers, which essentially consist of four pyranometers that measure total downward and upwelling shortwave and near-IR fluxes. The visible albedo was derived from the measurements of shortwave and near-IR. It is important to measure surface reflectance spectra simultaneously with the satellite overpass over homogeneous plots of different cover types.

In a typical field campaign for surface reflectance measurements, we usually carried three ASD spectroradiometers at three different parts of our test site. During the period of the satellite overpass (± 1 h), each group with one ASD spectroradiometer measured surface reflectance over three or four homogenous fields (plots) with the typical size of

Fig. 2. Configuration of the albedometers in the field.

200–300 m in each side. In each field (plot), 50–100 points along several transects were measured. A white reference panel was measured every point or every few points, depending on the atmospheric conditions. The ASD spectroradiometer detector was held by hand in the nadir direction and operated in radiance mode. This device has a 22° field of view. The radiance readings of the target and the white panel can then be used to derive reflectance. We usually did not geolocate each point, but each field (plot) was located using a Global Positioning System (GPS) device and/or marked on a high-resolution air photo. The average reflectance of these points was used to represent the mean reflectance of that field (plot). As a result, we can obtain about 10 surface reflectance spectra of different cover types in each field campaign during the satellite overpass.

Albedometer measurements were made in two different ways. The first is from two albedometers mounted on a 10-m tower over a field near the center of the study area. These measurements are taken every 10 min. Other measurements were made from two additional albedometers mounted at the top of a tripod or a ladder (about 2 m high). These portable albedometers take albedo measurements every 1 min and could be moved from one cover type to another during the overpass window. We also moved an ASD spectroradiometer along with the albedometers to make the simultaneous measurement of surface reflectance. The data collected around the satellite overpass were used to calibrate broadband albedo products from ETM+, which were then aggregated to validate the MODIS albedo products. Otherwise, the measured reflectances and albedos that

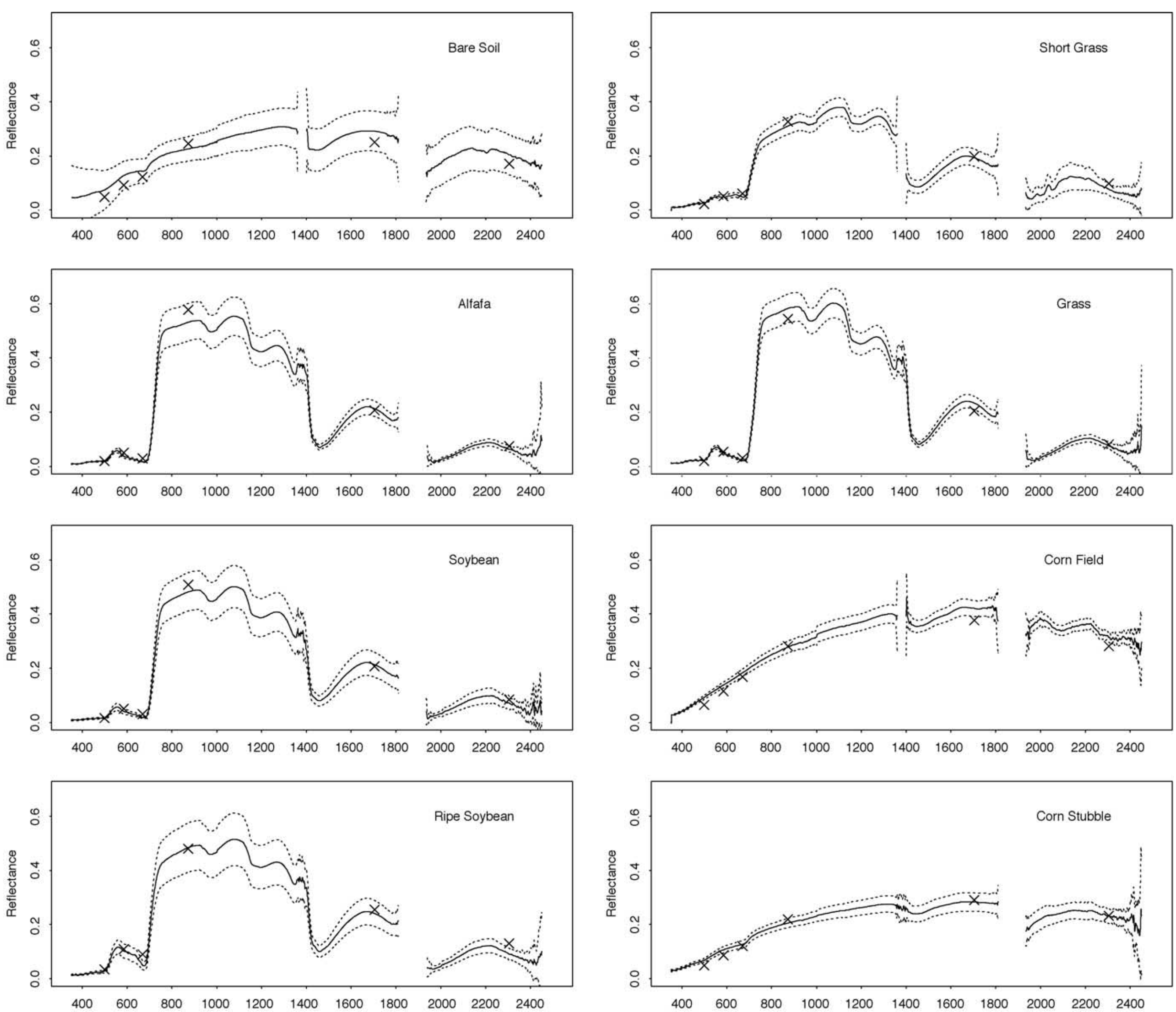

Fig. 3. Validating retrieved surface reflectance of atmospherically corrected ETM+ imagery by using ground simultaneous measurements. Dark points represent the retrieved ETM+ reflectance, solid line and two dash lines represent mean and one standard deviation of the measured surface reflectance spectra. Gaps resulted from extremely high instrument noises.

were collected simultaneously were used to validate the conversion formulae of narrowband to broadband albedos.

3. Validation methodology

If a surface is very homogeneous and large enough relative to the MODIS pixel size, a simple validation method might be to make multiple point measurements in the field and then compare the average reflectance/albedo of these points with the MODIS products. Considering various errors due to navigation or registration, the field has to be as large as several MODIS pixels. There is not such a large homogeneous field over BARC and many other test sites around the world.

Our validation approach is to scale up the point measurements to the MODIS resolution using high-resolution ETM+ imagery. There are three key technical steps in this procedure. The first is the atmospheric correction of ETM+ imagery that converts the top of atmosphere (TOA) radiance to surface reflectance. The second is to convert narrowband to broadband albedos. The third is to scale up from ETM+ resolution (30 m) to the MODIS resolution (250–1000 m). All these issues have been discussed in separate papers (Liang, 2000, 2001; Liang, Fang, & Chen, 2001). The focus of this paper is to combine these methods with other procedures to form our validation methodology and then apply this methodology to evaluate the MODIS products. Before discussing the validation results, the major technical issues in our validation methodology will be briefly outlined.

3.1. Atmospheric correction

High-resolution satellite imagery (e.g., ETM+) represents the measurement of TOA radiance. To compare the measured surface reflectance spectra with satellite observations, we need to derive surface reflectance from the TOA radiance through some atmospheric correction procedure. There exist many algorithms in the literature for atmospherically correcting high-resolution imagery (particularly Thematic Mapper—TM imagery), including invariant object (Hall, Strebel, Nickeson, & Goetz, 1991), histogram matching (Richter, 1996), dark object (Kaufman et al., 1997; Liang et al., 1997; Ouaidrari & Vermote, 1999; Santer, Carrere, Dubuisson, & Roger, 1999; Teillet & Fedosejevs, 1995), contrast reduction (Tanre, Deschamps, Devaux, & Herman, 1988), and many other statistical methods (e.g., Lavreau, 1991; Porter, 1984; Switzer, Kowalik, & Lyon, 1981). To overcome the major limitations associated with these methods (e.g., required existence of dense vegetation canopies across the scene, requiring the same proportions of different cover types in the hazy and clear regions), we recently developed a new atmospheric correction method that can be used for correcting ETM+ imagery under any general atmospheric and surface conditions (Liang et al., 2001).

The basic idea of this new atmospheric correction algorithm presented in our first paper is to match histograms of each cover type between the clear and hazy regions in the first three visible bands (1, 2 and 3) where atmospheric scattering dominates. Each cover type is determined from a cluster analysis using three near-infrared

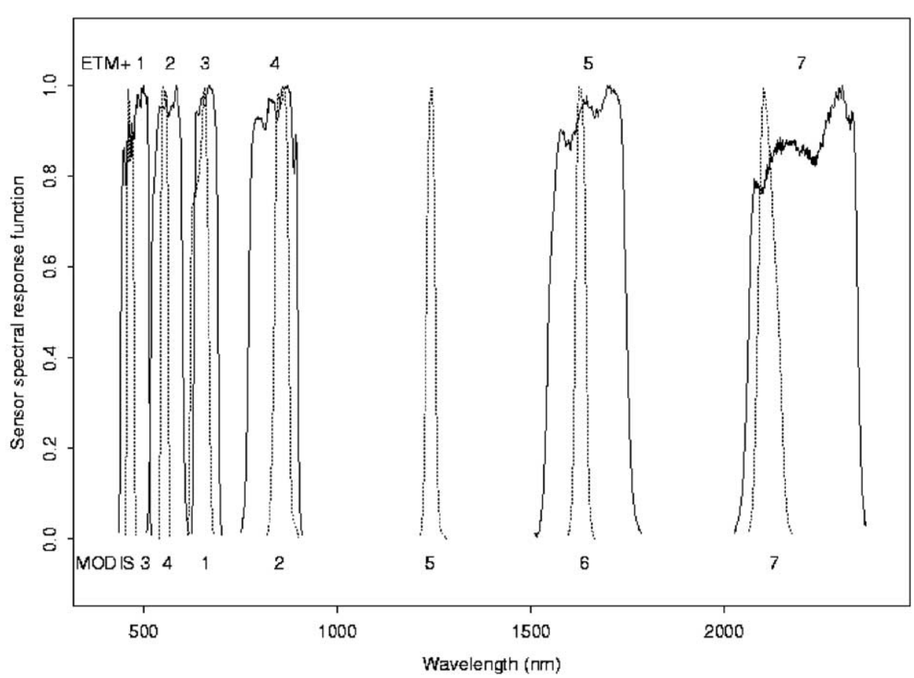

Fig. 4. MODIS and ETM+ shortwave spectral response functions.

and middle-infrared bands (ETM+ bands 4, 5 and 7) in which aerosol scattering is usually relatively weak. If the haze is indeed severe or there exist some thin clouds in the image, these three bands are also affected and a histogram matching is performed for these three bands before the cluster analysis is performed. Because of the high spatial resolution of ETM+ imagery, the surface adjacency effect is also taken into consideration in the atmospheric correction algorithm. An analytical formula was developed based on extensive simulations using a three-dimensional radiative transfer model. Given the aerosol optical depth and other ancillary information, surface reflectance is retrieved by searching the look-up tables that were created by MODTRAN.

For validation purposes at our test site, we corrected clear ETM+ imagery using the measured aerosol optical depths and water vapor content from Sunphotometers. If the image is heterogeneously hazy, the aerosol estimation mode of our atmospheric correction code was turned on and the estimated aerosol optical depth was calibrated by the measured sunphotometer values. The ground-measured reflectances were used to calibrate the retrieved surface reflectances by applying a linear regression equation to each band.

The output of the ETM+ atmospheric correction procedure is the surface reflectance for six spectral bands. After being calibrated by the ground measurements, they can be aggregated to the MODIS resolution to either validate the MODIS bidirectional reflectance product (MOD09) or to convert to broadband albedos for validating MODIS broadband albedo products.

3.2. Narrowband to broadband albedo conversion

If a surface is assumed to be Lambertian, the retrieved surface reflectance of different spectral bands are equivalent to surface spectral albedos. A follow-up step is to convert these narrowband albedos to broadband albedos in order to validate MODIS broadband albedos. Studies on the narrowband to broadband albedo conversions in the literature (e.g., Brest & Goward, 1987; Duguay & LeDrew, 1992; Gratton, Howart, & Marceau, 1993; Knap, Reijmer,

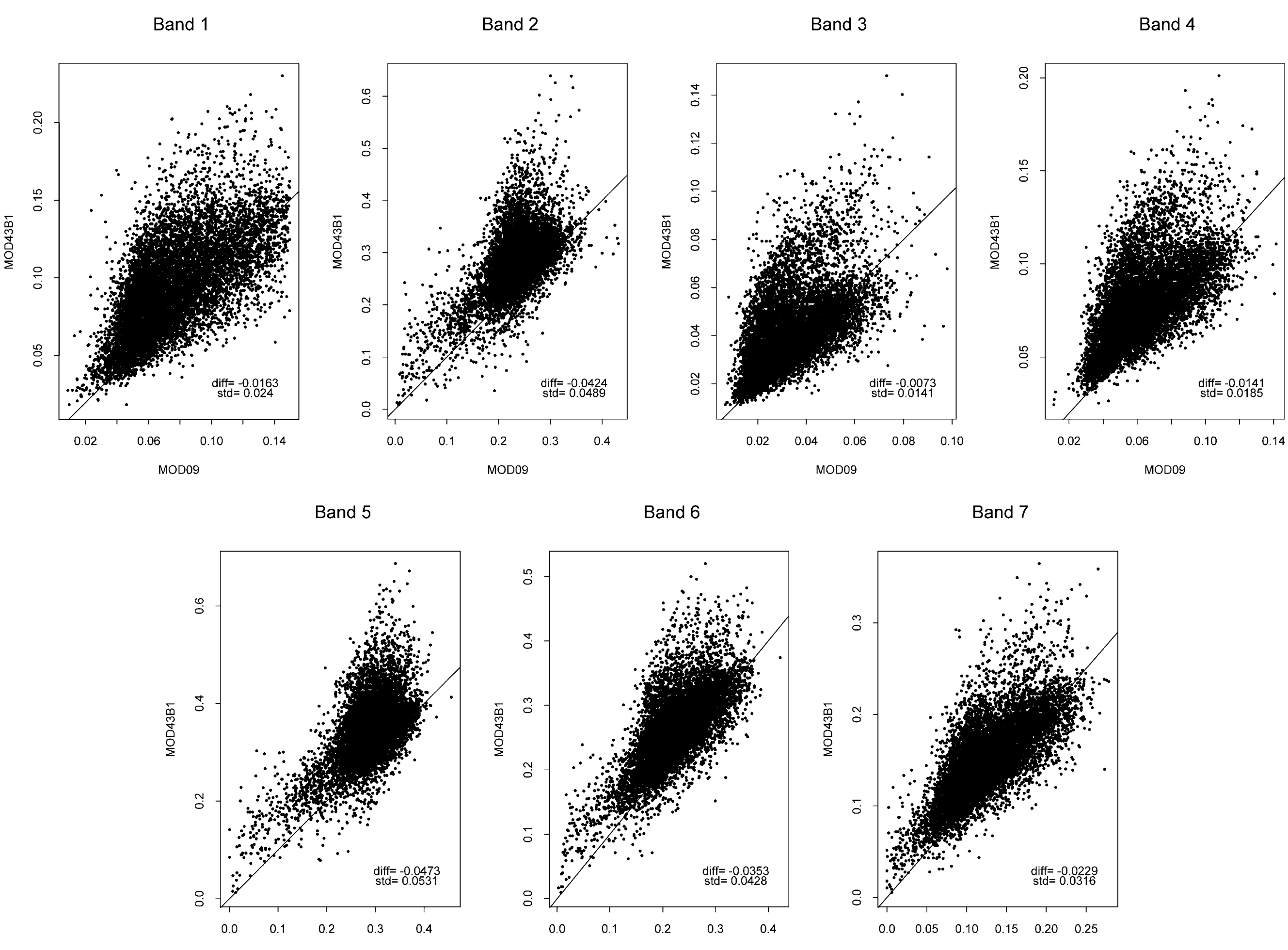

Fig. 5. Validating MODIS surface bidirectional reflectance product (MOD09).

& Oerlemans, 1999) are based on either field measurements of certain surface types or model simulations with a limited number of inputs. Existing research is also primarily oriented towards calculating total shortwave broadband albedo. Based on extensive radiative transfer simulations, Liang (2001) recently develop the conversion formulae of several sensors for calculating seven broadband albedos (total-shortwave, -visible and -near-IR, direct- and diffuse-visible and -near-IR), including ASTER, AVHRR, ETM+/TM, GOES, MODIS, MISR, POLDER, and VEGETATION. The reflectance spectra used in the simulations are from a variety of surface types with the Lambertian assumption. The validation results (Liang et al., 2002) indicate an excellent agreement between the predictions by these formulae and ground measurements. The average residual error (RSE) of predicted broadband albedos for most sensors including ETM+ are about 0.02. For easy reference, the formulae for calculating three broadband albedos from ETM+/TM spectral albedos α_i are given below:

$$\alpha_{short} = 0.356\alpha_1 + 0.13\alpha_3 + 0.373\alpha_4 + 0.085\alpha_5 + 0.072\alpha_7$$

$$\alpha_{vis} = 0.443\alpha_1 + 0.317\alpha_2 + 0.240\alpha_3$$

$$\alpha_{NIR} = 0.693\alpha_4 + 0.212\alpha_5 + 0.116\alpha_7$$

Note that most reflectance spectra used in the simulations are from the “natural surfaces” (e.g., vegetation, soil, and water). At the ETM+ and MODIS spatial resolutions, most pixels are mixed by these natural surfaces. An important question is whether the conversion formulae from the natural surfaces are suitable for the mixed surfaces. Since most conversion formulae are linear and if we assume that the linear mixing principle is valid, as

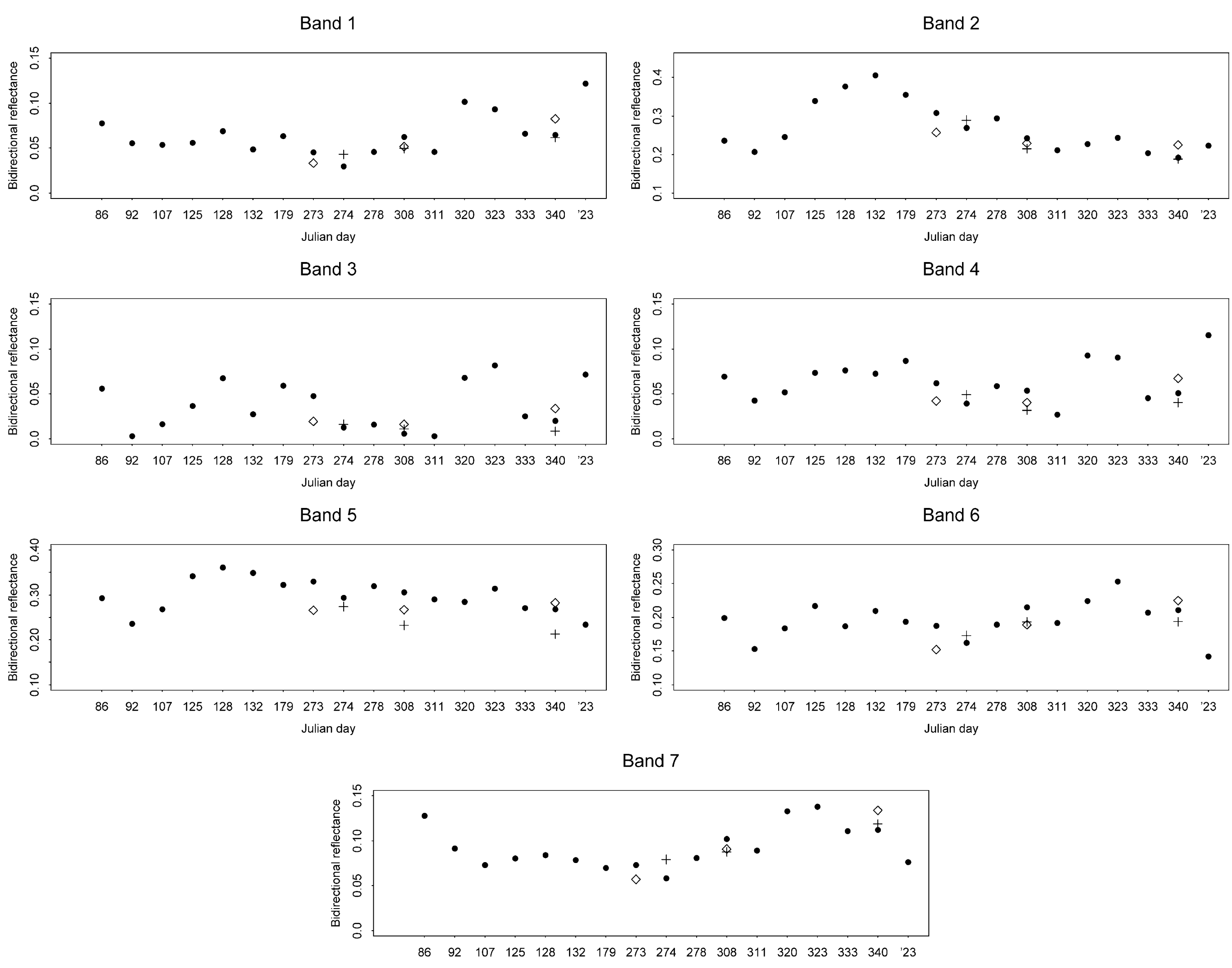

Fig. 6. Comparing the retrieved surface spectral directional reflectance (solid sphere) from MODIS level 1 products using the measured aerosol optical depths and water vapor content with MOD09 product (diamond) and the retrieved surface reflectance from ETM+ (plus).

demonstrated by many studies on linear unmixing, the answer to this question is affirmative. It is in fact verified by our validation study (Liang et al., 2002) in which many surface types are mixed.

3.3. Registration and aggregation

After "calibrating" the high-resolution ETM+ surface reflectance and broadband albedo products, we need to aggregate them into the MODIS resolutions. There are two major issues associated with this process: registration and aggregation. Imagery registration at two quite different spatial resolutions is not trivial, particularly using an automatic registration procedure. Fortunately, validation does not necessarily require any automatic registration procedure since no large volume of satellite imagery needs to be processed operationally. Modern image processing packages provide us with sufficient advanced functions that allow us to register images with similar spatial resolutions effectively by visually selecting ground control points.

Scaling high-resolution reflectance and albedo products into the coarse resolutions is another tough problem because of the nonlinearity in this process. When the atmosphere is not perfectly clear and surface reflectance is not too low, the multiple interaction between the atmosphere and surface is a nonlinear process. As a result, the dark surface objects look brighter and bright surface objects look darker in a neighboring region. This is usually called the adjacency effect. Therefore, the apparent reflectance of a neighboring region is not a linear average of the reflectance of each surface in general. Although many simplified algorithms have been developed to account for the adjacency effect (Kaufman, 1989), an accurate simulation has to rely on three-dimensional models. In a recent study, Liang (2001) conduct an extensive simulation study using a three-dimensional atmospheric radiative transfer model and found that upscaling of reflectance and albedo products from the 30 m resolution (ETM+) to the 1000 m resolution (MODIS) is highly linear. It implies that we can linearly average the ETM+ reflectance and albedo products of 30 m to the MODIS products of

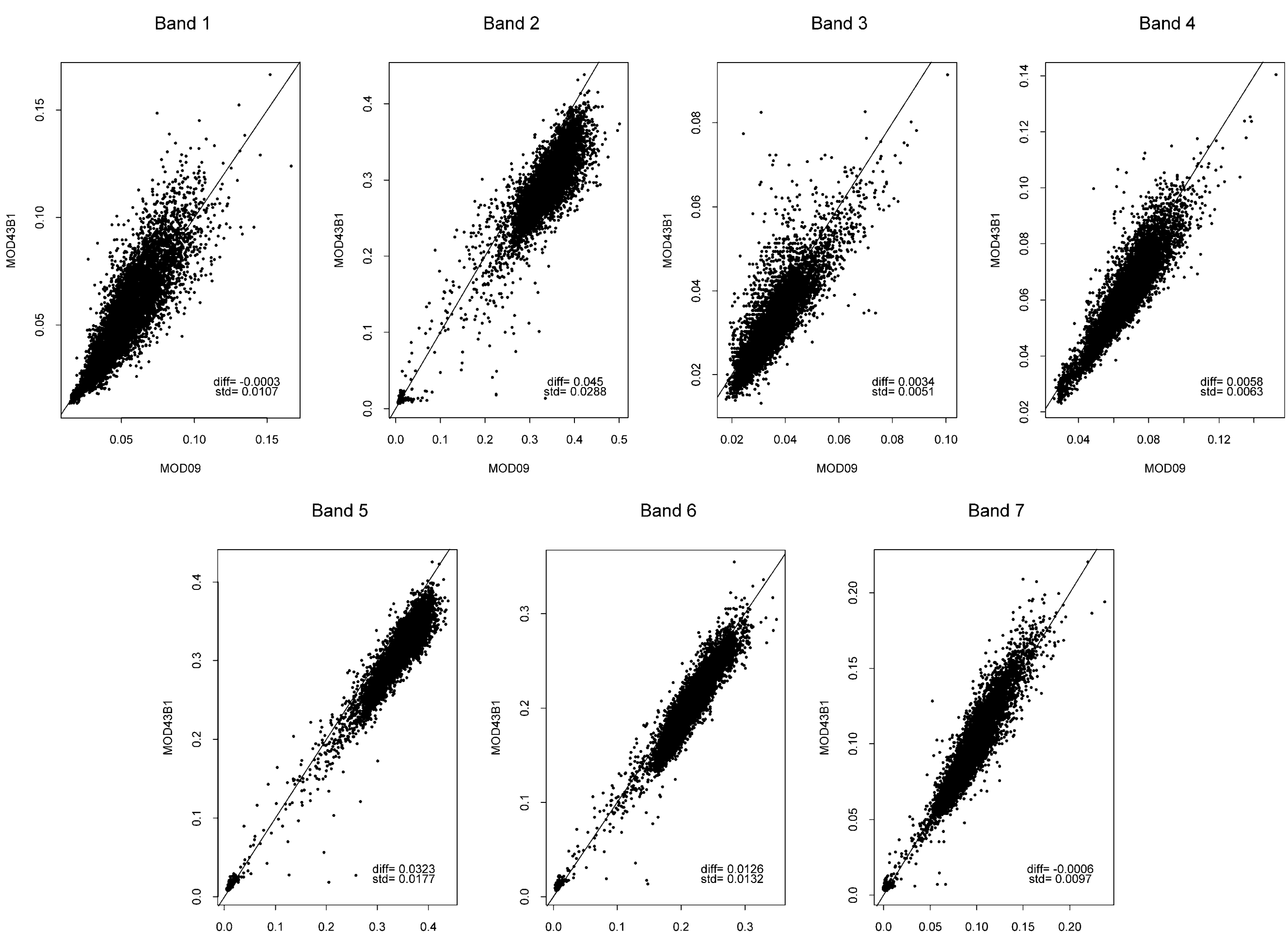

Fig. 7. Comparisons of MOD09 (directional reflectance from atmospheric correction) with predicted directional reflectance from MODIS BRDF parameters (MOD43B1) on September 29, 2000.

1000 m without introducing any significant amount of errors. Note that this simulation result is only suitable for scaling from 30 to 1000 m for our particular validation purpose here. Intuitively, it might be suitable for scaling from higher resolution (smaller than 30 m) to 1000 m. However, it is not a universal conclusion suitable for scaling of any resolutions (e.g., scaling from 1 to 5 m).

We need to point out that a major limitation in these methods is the assumption of a Lambertian surface. The reason for making such an assumption is that we do not have a good understanding of anisotropic reflectance at the landscape scale at this point. This limitation can be overcome in the near future with the availability of multiangular observations, such as MISR data.

4. Preliminary validation results

4.1. ETM+ imagery and data processing

Two clear-sky ETM+ images were collected over our test site at Beltsville, MD (path 15/row 33, October 2, 2000 and November 3, 2000). The solar zenith angles for the ETM+ images were 46.57° and 56.91°, respectively, and for the associated MODIS images the solar zenith angles were 44.66° and 54.87°, respectively. The new atmospheric correction algorithm (Liang et al., 2001) was used to derive surface reflectance with the inputs from Sunphotometer measurements of aerosol optical depths and water vapor content. On October 2, 2000, ground measurements of reflectance spectra of different cover types were made with the Landsat7 and Terra overpasses. The retrieved ETM+ reflectance is found to be in very good agreement with the measured reflectance spectra of several cover types (Fig. 3). In almost every case, the ground measured reflectance is within 5% of ETM+ derived reflectances (relative error). There still exist some differences, which may be the result of surface heterogeneity and other factors. Overall, the agreement is quite good. The retrieved surface reflectance images were adjusted by a linear equation based on these point measurements for each band. This procedure essentially is a calibration or validation of ETM+ reflectance product using ground "point" measurements.

It is impossible for us to identify common ground control points from both ETM+ and MODIS imagery directly because of the huge difference of the spatial resolutions. Instead, a two-step procedure was implemented. The average of every 17×17 ETM+ pixels was first calculated to generate the intermediate product of the 510-m resolution. A registration of the aggregated ETM+ imagery of 510 m was then performed with the 1 km MODIS imagery by manually selecting the common ground control points. Fortunately, it is very easy to identify the ground control points around our test site because of the existence of rivers, coastal lines and other distinct ground features. One issue is the determination of the origin of the grid of 17×17 pixels. When the results with three different origins (1,1), (4,4) and (8,8) were compared, their differences were quite small. Even so, the results presented below were based on their average.

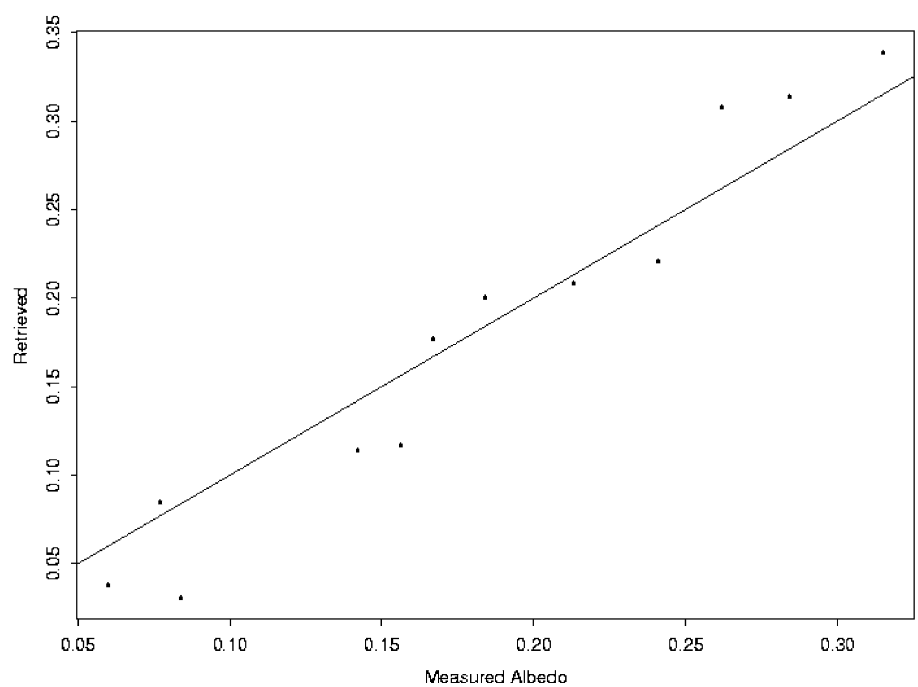

Fig. 8. Comparing the converted three broadband albedos from ETM+ imagery around the tower on four dates with albedometer measurements installed in the tower.

4.2. Validating surface directional reflectance (MOD09)

MODIS observations are acquired at many different viewing directions. It is not feasible to validate its directional reflectance using nadir-view ETM+ imagery. Since Landsat7 and Terra on which ETM+ and MODIS are respectively boarded are in the same orbit about 45 min apart, the MODIS imagery over our test site at Beltsville, MD are acquired on the same day as ETM+, which has very small viewing angles (very close to the nadir direction). Thus, the aggregated ETM+ surface reflectance can give us some indication of the accuracy of the MODIS reflectance products that are close to the nadir-viewing direction.

However, since both MODIS and ETM+ bands do not have exactly the same spectral response functions, we cannot make the direct comparisons. Fig. 4 shows their spectral response functions. They are quite different, and MODIS band 5 does not match any ETM+ bands at all. Statistical relations have been established instead based on hundreds of surface reflectance spectra of different cover types from our earlier study (Liang, 2001). These reflectance spectra were integrated with both MODIS and ETM+ sensor spectral response functions and a simple linear regression was then performed. The empirical formulae are to predict MODIS spectral band reflectance R_i from ETM+ spectral band reflectance (r_i):

$$R_1 = 0.0798r_2 + 0.9209r_3$$

$$R_2 = 0.1711r_1 - 0.2007r_2 + 1.0107r_4 + 0.0427r_5$$

$$R_3 = 1.0848r_1 - 0.1115r_2 + 0.0186r_3 + 0.0102r_4 - 0.0138r_5$$

$$R_4 = 1.1592r_2 - 0.1783r_3 + 0.0191r_4$$

$$R_5 = 0.5191r_1 - 0.7254r_2 + 0.7126r_4 + 0.5719r_5$$

$$R_6 = -0.0246r_4 + 1.1889r_5 - 0.1846r_7$$

$$R_7 = -0.1061r_1 + 0.1145r_2 - 0.0554r_4 + 0.0944r_5 + 0.9582r_7$$

The average residual errors of the predicted reflectances are smaller than 0.01. Some readers may wonder why MODIS band i reflectance R_i also depends on reflectances of several other ETM+ bands. The explanation is quite simple. If both MODIS and ETM+ had the identical spectral response functions, the coefficient of r_i would be 1, and the coefficients of other terms would be 0. When we conducted the simple linear regression between the corresponding bands only, we obtained similar results (i.e., slope and intercept are close to 1 and 0). However, the regression residuals were very large in many cases. To reduce the residuals, we have to take advantage of additional information (e.g., the possible correlation between visible and near-IR reflectance). This is the reason that we incorporated multiple ETM+ band reflectances including both visible and near-IR bands to predict each MODIS band reflectance in the above regression formulae.

The weather at our test site on October 2, 2000 was quite unstable. It was very clear for the Landsat7 overpass, but lots of cloud patches showed up shortly after for the Terra overpass. Clear MODIS imagery closest to October 2 was acquired on September 29. It is appropriate to compare MOD09 and ETM+ predicted reflectance on the same day. The comparison on November 3, 2000 is shown in Fig. 5. The standard deviation of the reflectance value differences are; Band 1: 0.024; Band 2: 0.049; Band 3: 0.014; Band 4: 0.019; Band 5: 0.053; Band 6: 0.043; and Band 7: 0.032. This indicates a possible insufficient aerosol correction or calibration problem associated with the MODIS data products.

One of the error sources of the MOD09 product is the inaccurate atmospheric input parameter, mainly aerosol optical depths and water vapor content. Fortunately, there are Sunphotometers installed at NASA/GSFC in our test site as part of the AERONET (Holben et al., 1998) whose measurements can be used for validating MOD09 product.

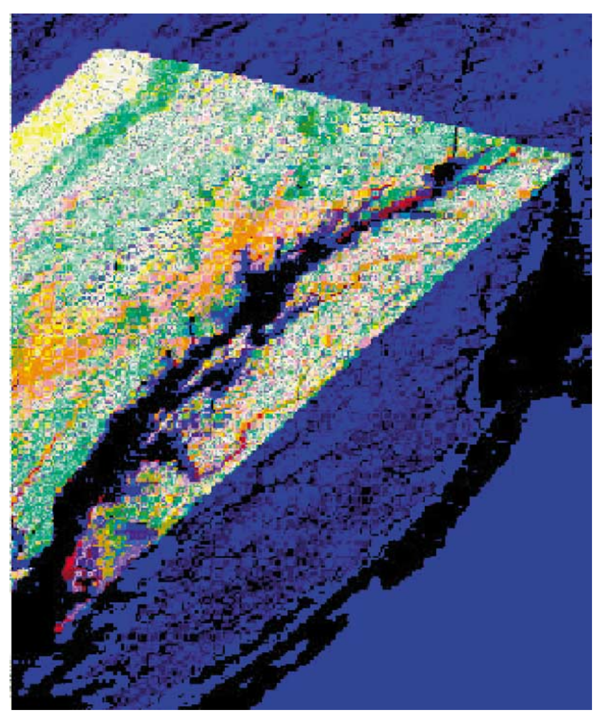

Fig. 9. Illustration of the registration of the aggregated ETM+ albedo products with MODIS albedo products. MODIS shortwave broadband albedo in blue, the aggregated ETM+ shortwave and visible albedos in green and red. The smaller region in the upper left corresponds to the ETM+ imagery.

We extracted a 3 × 3 window from each MODIS level 1b product acquired at different times and corrected these pixels using the measured aerosol optical depth and water vapor content using the look-up tables created by MODTRAN. The corrected surface spectral bidirectional reflectance (solid sphere) and MOD09 products are compared in Fig. 6. There are only three MOD09 points (diamond) in this figure, more data points will be provided by the MODIS processing team. The corresponding ETM+ surface reflectances are also presented in the same figure (plus). The comparison looks very good. The standard deviation of the differences between the retrieved ETM+ surface reflectance using Sunphotometer data and MOD09 products for these seven bands are: 0.015, 0.035, 0.012, 0.017, 0.039, 0.027, and 0.019. Note that these days when MOD09 products are available had very clear sky conditions.

4.3. Validating surface BRDF

Validating surface BRDF is very challenging, particularly with the nadir-viewing ETM+ imagery. It is our ongoing research activity to validate MODIS surface BRDF product using multiangle measurements. MODIS BRDF product (MOD43B1) provides us with a set of coefficients that can be used for predicting reflectance at any given solar-viewing geometry. These coefficients are generated from the derived surface reflectance (MOD09) over 16 days if there are enough clear-sky observations available. As an exercise to check consistency, we compared the derived surface reflectance from atmospheric correction (MOD09) with the predicted bidirectional reflectance using the MODIS BRDF product. Any significant difference will indicate the possible errors in the processing chain. Fig. 7

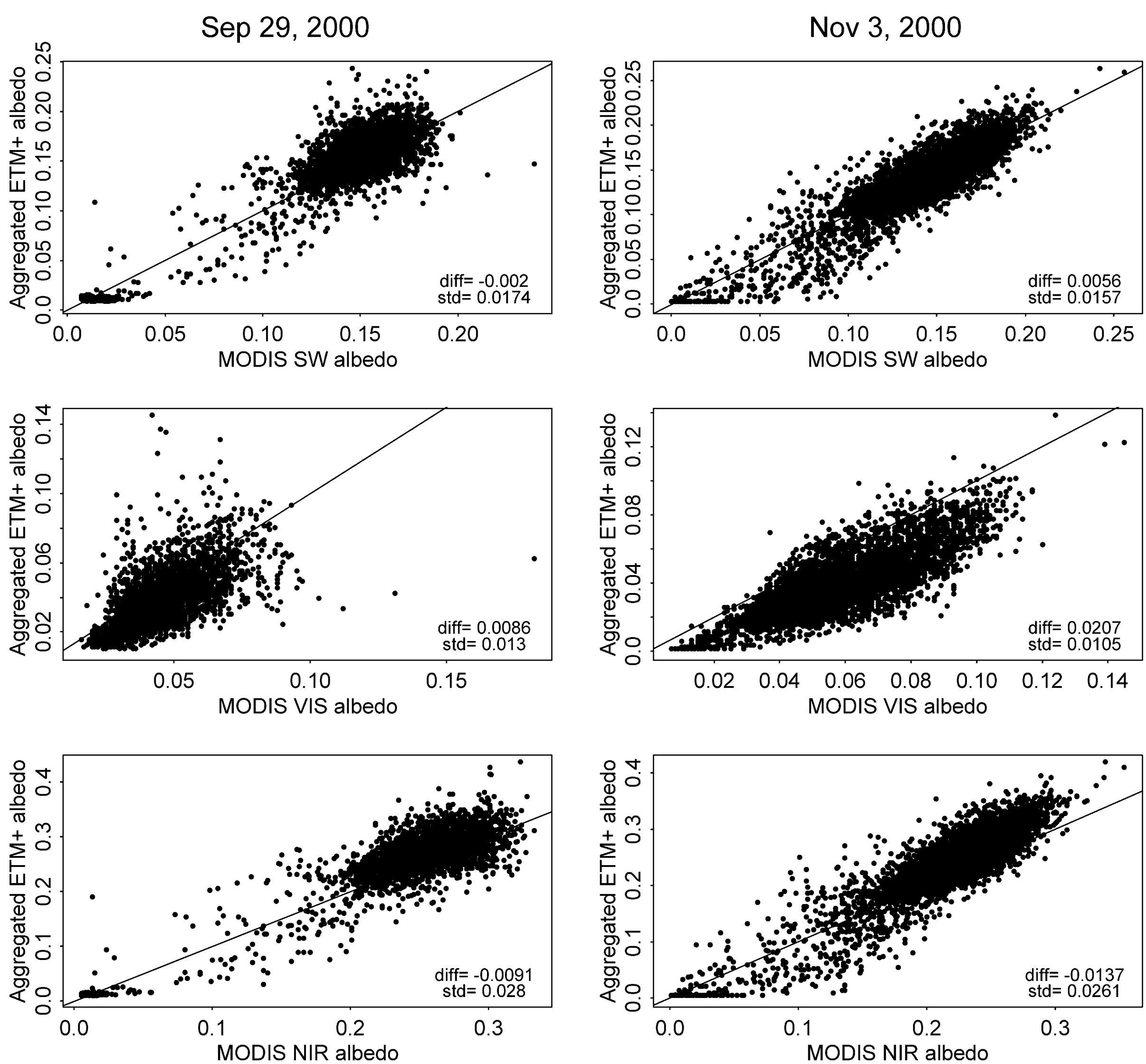

Fig. 10. Validating MODIS "black-sky" surface broadband albedo products (MOD43B3). SW, VIS and NIR represent total shortwave, visible and near-IR, respectively.

shows the comparison results on September 29, 2000. The standard deviation of the reflectance value differences are; Band 1: 0.011; Band 2: 0.029; Band 3: 0.005; Band 4: 0.006; Band 5: 0.018; Band 6: 0.013; and Band 7: 0.009. These differences may be explained by the fact that the MODIS BRDF parameters (MOD43B1) are fitted from the observed data during 16-day period, while MOD09 directional reflectance is an instantaneous product.

4.4. Validating surface broadband albedos

Land surface broadband albedo is a critical variable affecting the earth's climate. It has been well recognized that surface albedo is among the main radiative uncertainties in current climate modeling. Validating MODIS surface "black-sky" broadband albedos is straightforward given the discussion of the algorithms in the previous section. The derived surface spectral reflectance from ETM+ imagery is converted into these three broadband albedos based on the formulae (Liang, 2001) that have been validated using ground measurements (Liang et al., 2002). To verify the accuracy of the converted broadband albedo products, we extracted a 5×5 window from each ETM+ image around the tower where two albedometers are located. The converted average broadband albedos from ETM+ imagery are compared with albedometer measurements in Fig. 8 on four dates (September 29; October 2, December 5, 2000, and January 22, 2001). There are some differences (The largest differences are as large as 0.05), but the average difference is smaller than 0.02. The scale mismatch may account for some of the errors since albedometers in the tower are measuring albedos in a much larger area than a 5×5 ETM+ window represents.

The calculated broadband albedos from ETM+ were aggregated into the 510 m resolution and then registered with the MODIS broadband albedo products. The registration of these two images is illustrated in Fig. 9. The visual examinations reveal that these two images are matched very well. The quantitative comparisons are shown in Fig. 10.

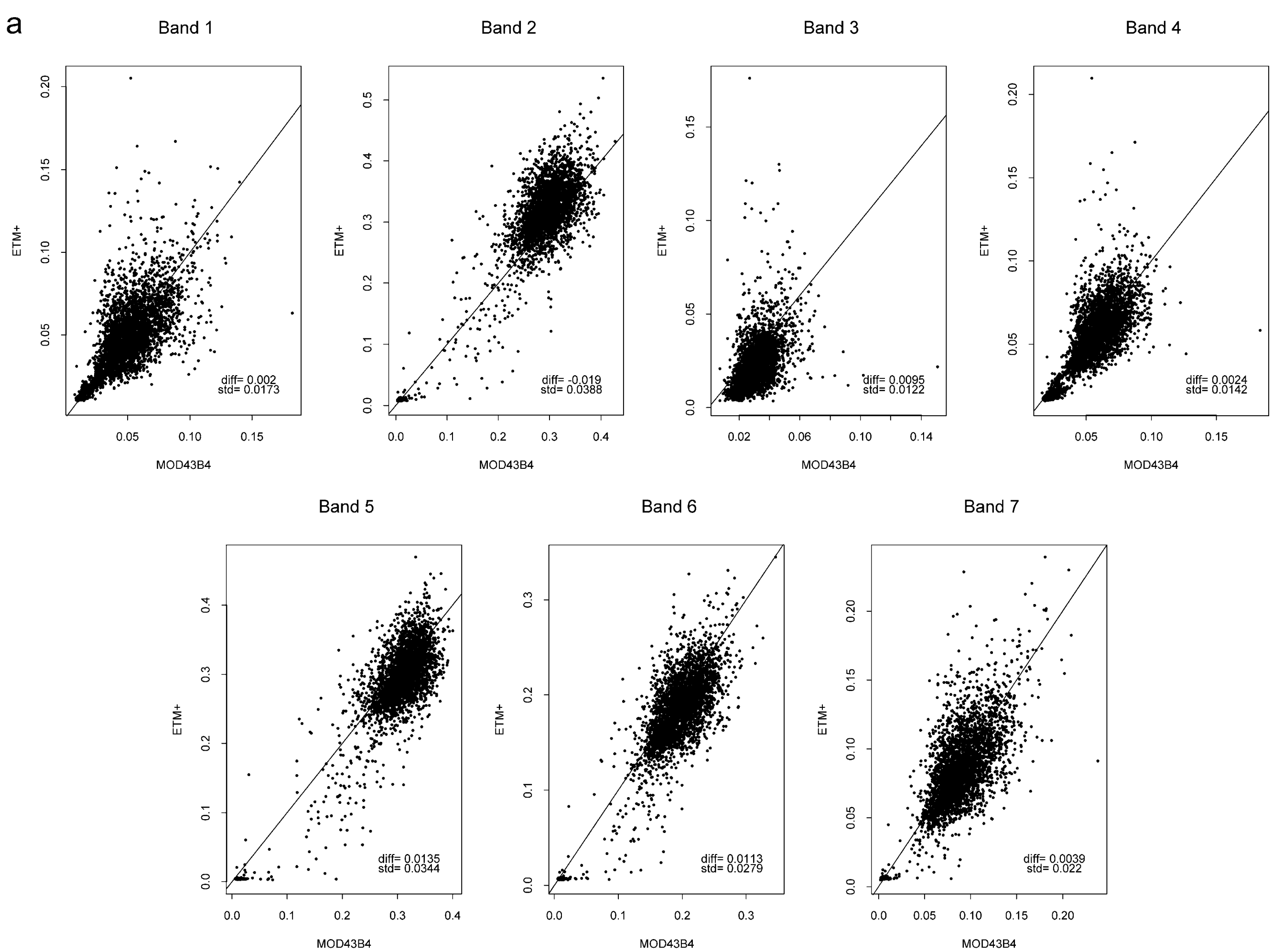

Fig. 11. Validating MODIS BRDF-adjusted surface nadir reflectance (MOD43B4) using the ETM+ imagery of October 2, 2000 (a) and November 3, 2000 (b). diff shows the mean difference between MOD43B4 and ETM+ aggregated reflectance, and std 1 standard deviation.

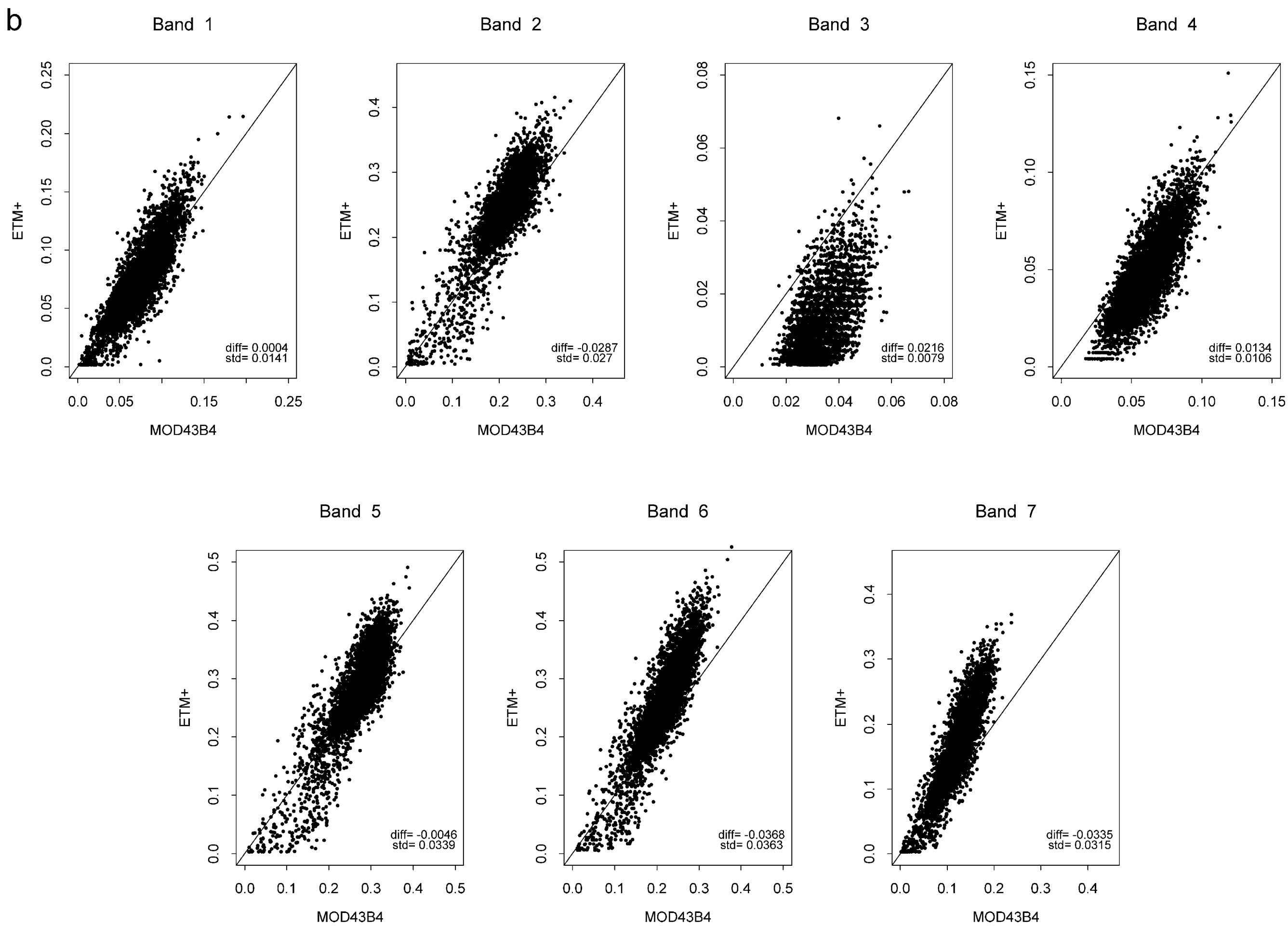

Fig. 11 (*continued*).

The MODIS "black-sky" broadband albedo product covers the 16-day period around September 29 and November 3, 2000. In the MODIS product, the mixing pixels along the coast are marked and assigned a maximum value (we changed to zero in this study), but we did not mark any mixed pixels from ETM+ imagery. This explains the vertical feature corresponding to zero MODIS albedo value in all figures.

The differences on the visible broadband albedos are the largest. The larger MODIS visible albedo values on both dates indicate the possible insufficient aerosol correction. Near-IR values match very well. The total shortwave albedo values on September 29, 2000 are very close with the mean difference -0.002 and standard deviation 0.017, although slightly larger MODIS shortwave albedo on November 3, 2000 is evident (the mean difference is 0.0056). The MODIS visible albedo on November 3 is also smaller than that from ETM+, but the mean difference is 0.0207 with the standard deviation of 0.0105. Overall, their comparisons are very good. We also want to point out that the MODIS "black-sky" albedo product reflects the 16-day average condition and is normalized to the local noon solar zenith angle. All these factors may contribute to these differences.

4.5. Validating nadir BRDF-adjusted surface reflectance

MOD43B4 is the equivalent nadir-viewing surface reflectance from directional observation after the BRDF adjustment (Schaaf et al., 2002, this issue). ETM+ imagery with the near nadir-viewing geometry is an excellent source for its validation.

Fig. 11 shows the comparisons of the MODIS product with our aggregated ETM+ products on both dates. On November 3, 2000, MODIS bands 3 (blue) and 4 (green) reflectance are much larger probably because of the insufficient aerosol correction and/or sensor calibration, but other bands show very good agreements of less than 0.01. Although there are large scatters in these plots, they contain 5000–10,000 pixels each. The mean differences and standard deviations are quite small. Note MOD43B4 represents 16-day average reflectance around these 2 days. Further work is planned to examine those pixels that have large deviations.

5. Discussion and conclusion

The validation of the MODIS land surface products has to rely on ground measurements. However, the direct comparison of ground "point/plot" measurements with MODIS products of up to 1 km is not feasible over most natural landscapes. The key issue in the MODIS product validation is the upscaling process from ground "point" measurements to MODIS resolutions using high-resolution remotely sensed imagery. Since high-resolution images measure the top-of-atmosphere radiance, a processing chain is needed to convert them into the similar land surface products in order to validate the corresponding MODIS land surface products. Therefore, validation is not limited to field measurements, algorithm development and refinement. Instead, ground measurements are used to "calibrate" high-resolution products that are then aggregated into the MODIS resolution. Thus, ground measurements are indirectly used for validating the MODIS land surface products.

In this study, Landsat7 ETM+ imagery were used to scale-up ground measurements to the MODIS resolutions for validating the MODIS land surface products. Three algorithms have been applied to develop the land surface products from ETM+ imagery in this study: atmospheric correction, narrowband to broadband albedo conversion, and spatial scaling. Field campaigns were conducted in Beltsville, MD, one of 24 EOS Land Core Validation Sites. Ground measurements were used to "calibrate" high-resolution products from ETM+ imagery, which were then aggregated to the MODIS resolutions for the direct comparisons with the MODIS land surface products.

Four MODIS products have been examined in this study, including (1) surface reflectance from atmospheric correction, (2) BRDF, (3) broadband albedos, and (4) nadir-viewing equivalent reflectance with the BRDF adjustment. The initial validation results show that these products are reasonably accurate (less than 5% absolute error). Since the MODIS products we used in this study are not the final ones, the final conclusion about the uncertainties of these products will be made after the MODIS data reprocessing. Note that the initial validation results were based on two clear days and the near nadir-viewing geometry over land surfaces that are mostly vegetated. If the atmospheric conditions are hazy or the surfaces are not vegetated, the MODIS atmospheric correction algorithm that relies on the dense vegetation may introduce error in the high-level products. The detailed validation activities for these conditions are currently under way.

In the current validation procedure, the surface has been assumed to be a Lambertian. This assumption was used in atmospheric correction and narrowband to broadband albedo conversion because we have not been able to determine surface BRDF properties at the ETM+ resolution. It is probably not a serious issue at this point since the MODIS atmospheric correction algorithm currently is also making such an assumption (Vermote, personnel communication), but it is certainly an important area to be improved in the future. We have recently acquired air-MISR data over our test site (July and August 2001) at similar and higher resolutions, which will greatly help us address this issue in the future.

The validation approaches presented in this paper are quite general and should be straightforward to be applied to other validation sites and/or validate the similar land surface products from other satellite systems.

Acknowledgements

The work is partially funded by NASA EOS validation program under grant NAG5-6459. Andy Russ and Wayne Dulaney contributed substantially to various field campaigns. The authors would like thank Dr. Eric Vermote for his helpful discussion of the MODIS products, Dr. Feng Gao for his help in handling the MODIS products, and particularly three anonymous reviewers for their careful reviewing and excellent comments that have significantly improved the presentation of this paper.

References

Brest, C. L., & Goward, S. (1987). Deriving surface albedo measurements from narrowband satellite data. *International Journal of Remote Sensing*, *8*, 351–367.

Duguay, C. R., & LeDrew, E. F. (1992). Estimating surface reflectance and albedo from Landsat-5 Thematic Mapper over rugged terrain. *Photogrammetric Engineering and Remote Sensing*, *58*, 551–558.

Gratton, D. J., Howart, P. J., & Marceau, D. J. (1993). Using Landsat-5 Thematic Mapper and Digital Elevation Data to determine the net radiation field of a mountain glacier. *Remote Sensing of Environment*, *43*, 315–331.

Hall, F. G., Strebel, D. E., Nickeson, J. E., & Goetz, S. J. (1991). Radiometric rectification: toward a common radiometric response among multidate, multisensor images. *Remote Sensing of Environment*, *35*, 11–27.

Holben, B. N., Eck, T., Slutsker, I., Tanre, T., Buis, J., Setzer, A., Vermote, E., Reagan, J., Kaufman, Y., Nakajima, T., Lavenu, F., Jankowiak, I., & Smirnov, A. (1998). AERONET—a federated instrument network and data archive for aerosol characterization. *Remote Sensing of Environment*, *66*, 1–16.

Justice, C., Starr, D., Wickland, D., Privette, J., & Suttles, T. (1998). EOS land validation coordination: an update. *The Earth Observer*, *10*(3), 55–60.

Justice, C. O., Vermote, E., Townshend, J. G. R., et al (1998). The Moderate Resolution Imaging Spectroradiometer (MODIS): land remote sensing for global change research. *IEEE Transactions on Geoscience and Remote Sensing*, *36*, 1228–1249.

Kaufman, Y. J. (1989). The atmospheric effect on remote sensing and its correction. In G. Asrar (Ed.), *Theory and applications of optical remote sensing*. New York: Wiley.

Kaufman, Y. J., Wald, A., Lorraine, L., Gao, B., Li, R., & Flynn, L. (1997). Remote sensing of aerosol over the continents with the aid of a 2.2 μm channel. *IEEE Transactions on Geoscience and Remote Sensing*, *35*, 1286–1298.

Knap, W., Reijmer, C., & Oerlemans, J. (1999). Narrowband to broadband conversion of Landsat TM glacier albedos. *International Journal of Remote Sensing*, *20*, 2091–2110.

Lavreau, J. (1991). De-hazing Landsat Thematic Mapper images. *Photogrammetry Engineering and Remote Sensing*, *57*, 1297–1302.

Liang, S. (2000). Numerical experiments on spatial scaling of land surface albedo and leaf area index. *Remote Sensing Reviews*, *19*, 225–242.

Liang, S. (2001). Narrowband to broadband conversions of land surface albedo: I. Formulae. *Remote Sensing of Environment*, *76*, 213–238.

Liang, S., Fallah-Adl, H., Kalluri, S., JaJa, J., Kaufman, Y., & Townshend, J. (1997). Development of an operational atmospheric correction algorithm for TM imagery. *Journal of Geophysical Research*, *102*, 17173–17186.

Liang, S., Fang, H., & Chen, M. (2001). Atmospheric correction of Landsat ETM+ land surface imagery: I. Methods. *IEEE Transactions on Geoscience and Remote Sensing*, *39*, 2490–2498.

Liang, S., Shuey, C., Russ, A., Fang, H., Walthall, C., & Daughtry, C. (2002). Narrowband to broadband conversions of land surface albedo: II. Validation. *Remote Sensing of Environment*, (in press).

Morisette, J., Privette, J., & Justice, C. (2002). Moderate resolution imaging spectra radiometer land validation activities. *Remote Sensing of Environment*, 83, 77-96 (this issue).

Morisette, J., Privette, J., Justice, C., Olson, D., Dwyer, J., Davis, P., Starr, D., & Wickland, D. (1999). The EOS land validation core sites: background information and current status. *The Earth Observer*, *11*, 26.

Ouaidrari, H., & Vermote, E. (1999). Operational atmospheric correction of Landsat TM data. *Remote Sensing of Environment*, *70*, 4–15.

Porter, J. F. (1984). The channel correlation method for estimating aerosol levels from multispectral scanner data. *Photogrammetry Engineering and Remote Sensing*, *50*, 43–52.

Richter, R. (1996). A spatially adaptive fast atmospheric correction algorithm. *International Journal of Remote Sensing*, *17*, 1201–1214.

Santer, R., Carrere, V., Dubuisson, P., & Roger, J. C. (1999). Atmospheric correction over land for MERIS. *International Journal of Remote Sensing*, *20*, 1819–1840.

Schaaf, C., Gao, F., Strahler, A., Lucht, W., Li, X., Tsung, T., Strugnell, N., Zhang, X., Jin, Y., Muller, J.-P., Lewis, P., Barnsley, M., Hobson, P., Disney, M., Roberts, G., Dunderdale, M., Doll, C., d'Entremont, R., Hu, B., Liang, S., Previtte, J., & Roy, D. (2002). First operational BRDF, albedo and nadir reflectance products from MODIS. *Remote Sensing of Environment*, 83, 135-148 (this issue).

Strahler, A. H., Wanner, W., Schaaf, C., Li, X., et al. (1999). *MODIS BRDF/albedo product: ATBD*, Version 5.0, April, 1999.

Switzer, P., Kowalik, W., & Lyon, R. (1981). Estimation of atmospheric path-radiance by the covariance matrix method. *Photogrammetry Engineering and Remote Sensing*, *47*, 1469–1476.

Tanre, D., Deschamps, P., Devaux, C., & Herman, M. (1988). Estimation of Saharan aerosol optical thickness from blurring effects in Thematic Mapper data. *Journal of Geophysical Research*, *93*, 15955–15964.

Teillet, P. M., & Fedosejevs, G. (1995). On the dark target approach to atmospheric correction of remotely sensed data. *Canadian Journal of Remote Sensing*, *21*, 374–387.

Vermote, E. (1999). *Atmospheric correction algorithm: spectral reflectance*, MOD09 ATBD, May 1999.